ORGANIC LETTERS

2012
Vol. 14, No. 1
62–65

Synthesis and Properties of Isomerically Pure Anthrabisbenzothiophenes

Dan Lehnherr,[†] Rawad Hallani,[‡] Robert McDonald,[†,§] John E. Anthony,*[,‡,∥] and Rik R. Tykwinski*[,⊥,#]

Department of Chemistry, University of Alberta, Edmonton, Alberta, T6G 2G2, Canada, Department of Chemistry, University of Kentucky, Lexington, Kentucky 40506, United States, and Institut für Organische Chemie, Friedrich-Alexander-Universität, Erlangen-Nürnberg, Henkestrasse 42, 91054 Erlangen, Germany

rik.tykwinski@chemie.uni-erlangen.de; anthony@uky.edu

Received October 21, 2011

ABSTRACT

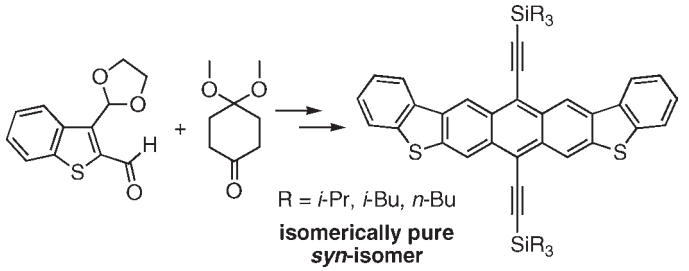

The synthesis of three heptacyclic heteroacenes is described, namely anthra[2,3-*b*:7,6-*b*′]bis[1]benzothiophenes (ABBTs). A stepwise sequence of aldol reactions provides regiochemical control, affording only the *syn*-isomer. The ABBTs are characterized by X-ray crystallography, UV−vis absorption, and emission spectroscopy, as well as cyclic voltammetry. Field effect transistors based on solution-cast thin films of ABBT derivatives exhibit charge-carrier mobilities of as high as 0.013 cm^2/(V s).

Over the past decade or so, there have been significant advances in the development of acene derivatives for semiconductor applications.[1] Studies of these new materials demonstrate remarkable potential for their use in, for example, organic field effect transistors and photovoltaics.[1] The formation of heteroacenes, through the formal incorporation of heteroatoms into a hydrocarbon acene skeleton, allows for tuning of electronic properties, as well as the realization of new chromophore structures.[2]

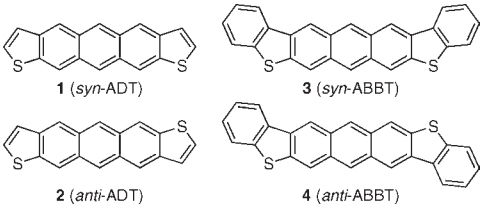

Figure 1. Structures of *syn*- and *anti*-ADT (**1** and **2**, respectively) and benzannulated relatives *syn*- and *anti*-ABBT (**3** and **4**, respectively).

Anthradithiophenes (ADTs, **1**−**2**, Figure 1) are a subclass of heteroacenes that often show promising semiconducting properties similar to that of pentacene.[3a] Furthermore,

[†] University of Alberta.
[‡] University of Kentucky.
[§] X-ray Crystallography Laboratory, Department of Chemistry.
[∥] Author to whom correspondence for device fabrication and characterization should be addressed.
[⊥] Friedrich-Alexander-Universität.
[#] Author to whom correspondence for molecule synthesis and characterization should be addressed.

(1) (a) Anthony, J. E. *Chem. Rev.* **2006**, *106*, 5028–5048. (b) Anthony, J. E. *Angew. Chem., Int. Ed.* **2008**, *47*, 452–483. (c) Bendikov, M.; Wudl, F.; Perepichka, D. F. *Chem. Rev.* **2004**, *104*, 4891–4945. (d) Lehnherr, D.; Tykwinski, R. R. *Aust. J. Chem.* **2011**, *64*, 919–929.

(2) (a) Hinsberg, O. *Liebigs Ann. Chem* **1901**, *319*, 257–286. (b) Miao, Q.; Nguyen, T. Q.; Someya, T.; Blanchet, G. B.; Nuckolls, C. *J. Am. Chem. Soc.* **2003**, *125*, 10284–10287. (c) Payne, M. M.; Delcamp, J. H.; Parkin, S. R.; Anthony, J. E. *Org. Lett.* **2004**, *6*, 1609–1612. (d) Payne, M. M.; Odom, S. A.; Parkin, S. R.; Anthony, J. E. *Org. Lett.* **2004**, *6*, 3325–3328. (e) Payne, M. M.; Parkin, S. R.; Anthony, J. E.; Kuo, C.-C.; Jackson, T. N. *J. Am. Chem. Soc.* **2005**, *127*, 4986–4987. (f) Chen, J.; Kampf, J. W.; Ashe, A. J., III. *Organometallics* **2008**, *27*, 3639–3641. (g) Appleton, A. L.; Brombosz, S. M.; Barlow, S.; Sears, J. S.; Bredas, J.-L.; Marder, S. R.; Bunz, U. H. F. *Nat. Commun.* **2010**, *1*, 91. (h) Niimi, K.; Shinamura, S.; Osaka, I.; Miyazaki, E.; Takimiya, K. *J. Am. Chem. Soc.* **2011**, *133*, 8732–8739.

10.1021/ol202843x
Published on Web 11/29/2011

when appropriately functionalized, ADTs normally show improved stability relative to pentacenes.[2e,3b,4] To date, however, ADT and its derivatives have typically been synthesized and studied as a mixture *syn*- and *anti*-isomers (**1** and **2**, respectively),[3] although the study of isomerically pure ADTs has recently been achieved in two cases.[5,6]

Scheme 1. Synthesis of *syn*-ABBTs **5a**–**c**

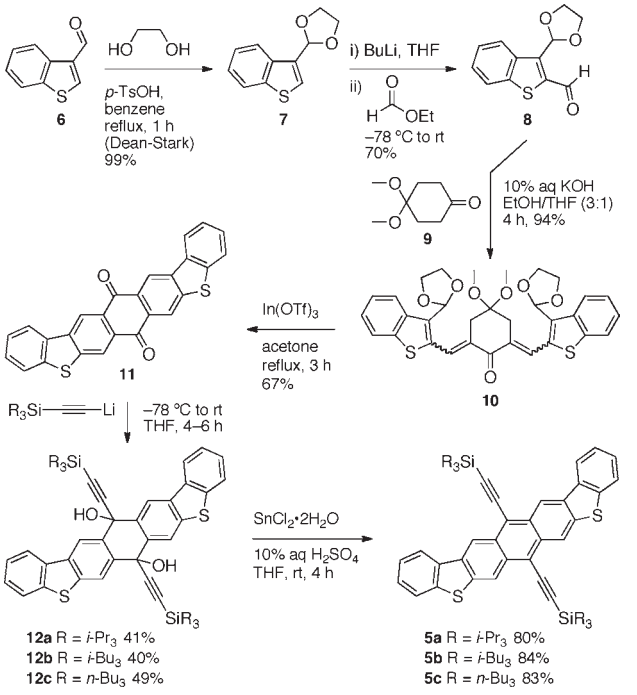

Intrigued by the performance of ADTs in semiconducting devices and challenged by the issue of obtaining isomerically pure chromophores that might offer decreased disorder compared to the isomeric ADT mixtures, we targeted the synthesis of a new class of ADT analogues, anthrabis[1]benzothiophenes (ABBTs, Figure 1). The additional aromatic ring at each benzothiophene moiety of the ABBTs results in a slightly bent or curved structure. It was thus expected that disordered solid-state packing observed for ADTs should be avoided for ABBTs via more discriminate interactions in the solid, based on both steric and electronic demands. Similar to ADTs, however, there are two possible isomers for ABBTs, the *syn*- and *anti*-isomers (**3** and **4**, respectively). In the present study, we report the selective synthesis and properties of *syn*-ABBTs **5a**–**c** (Scheme 1).

The synthesis of ABBTs **5a**–**c** began with commercially available thianaphthene-3-carboxaldehyde (**6**). Protection of the aldehyde as an acetal using 1,2-ethylene glycol afforded **7**. Lithiation of **7** followed by reaction with ethyl formate provided the masked dialdehyde **8** in 70% yield. A 2-fold aldol condensation of **9** with **8** provided intermediate **10** in 94% yield.[7] Global deprotection of the three acetal groups of **10** was accomplished with catalytic $In(OTf)_3$ (12 mol %) under reflux in acetone. These same conditions effected the subsequent intramolecular aldol condensation, leading to the one pot formation of quinone **11** in 67% yield from **10**.[8] Isolated as a brown solid, quinone **11** is sparingly soluble in common organic solvents. Nevertheless, reaction of **11** with various lithium acetylides could be accomplished in THF at low temperature and afforded diols **12a**–**c** in moderate yields. Aromatization was accomplished in the usual way with $SnCl_2 \cdot 2H_2O$ in the presence of 10% aq H_2SO_4, providing ABBTs **5a**–**c** in good yield.

Table 1. Thermal Properties of ABBTs **5a**–**c**

			DSC decomposition[a]	
compd	TGA T_d/°C[a]	DSC mp/°C[a]	onset/°C	peak/°C
5a	415	414	414	415
5b	360	319	347	360
5c	380	242	345	355

[a] Measured under nitrogen atmosphere.

ABBT **5a** has limited solubility in common solvents, while derivatives **5b**,**c** show much improved solubility because of the larger trialkylsilyl groups and can be easily dissolved in solvents such as THF, CH_2Cl_2, and $CHCl_3$. The constitution of the trialkylsilyl group also affects the thermal properties as assessed by differential scanning calorimetry (DSC) and thermogravimetric analysis (TGA, Table 1). *i*-Pr_3Si-substituted ABBT **5a** has the highest

(3) (a) Laquindanum, J. G.; Katz, H. E.; Lovinger, A. J. *J. Am. Chem. Soc.* **1998**, *120*, 664–672. (b) Subramanian, S.; Park, S. K.; Parkin, S. R.; Podzorov, V.; Jackson, T. N.; Anthony, J. E. *J. Am. Chem. Soc.* **2008**, *130*, 2706–2707. (c) Wang, J.; Liu, K.; Liu, Y.-Y.; Song, C.-L.; Shi, Z.-F.; Peng, J.-B.; Zhang, H.-L.; Cao, X.-P. *Org. Lett.* **2009**, *11*, 2563–2566. (d) Kim, C.; Huang, P.-Y.; Jhuang, J.-W.; Chen, M.-C.; Ho, J.-C.; Hu, T.-S.; Yan, J.-Y.; Chen, L.-H.; Lee, G.-H.; Facchetti, A.; Marks, T. J. *Org. Electron.* **2010**, *11*, 1363–1375. (e) Balandier, J.-Y.; Quist, F.; Stas, S.; Tylleman, B.; Ragoen, C.; Mayence, A.; Bouzakraoui, S.; Cornil, J.; Geerts, Y. H. *Org. Lett.* **2011**, *13*, 548–551. (f) Goetz, K. P.; Li, Z.; Ward, J. W.; Bougher, C.; Rivnay, J.; Smith, J.; Conrad, B. R.; Parkin, S. R.; Anthopoulos, T. D.; Salleo, A.; Anthony, J. E.; Jurchescu, O. D. *Adv. Mater.* **2011**, *23*, 3698–3703.

(4) (a) Kaur, I.; Jia, W.; Kopreski, R. P.; Selvarasah, S.; Dokmeci, M. R.; Pramanik, C.; McGruer, N. E.; Miller, G. P. *J. Am. Chem. Soc.* **2008**, *130*, 16274–16286. (b) Northrop, B. H.; Houk, K. N.; Maliakal, A. *Photochem. Photobiol. Sci.* **2008**, *7*, 1463–1468. (c) Li, Y.; Wu, Y.; Liu, P.; Prostran, Z.; Gardner, S.; Ong, B. S. *Chem. Mater.* **2007**, *19*, 418–423. (d) Maliakal, A.; Raghavachari, K.; Katz, H.; Chandross, E.; Siegrist, T. *Chem. Mater.* **2004**, *16*, 4980–4986. (e) Ono, K.; Totani, H.; Hiei, T.; Yoshino, A.; Saito, K.; Eguchi, K.; Tomura, M.; Nishida, J.-I.; Yamashita, Y. *Tetrahedron* **2007**, *63*, 9699–9704.

(5) For examples of the synthesis of isomerically pure ADTs, see: (a) Li, Z.; Lim, Y.-F.; Kim, J. B.; Parkin, S. R.; Loo, Y.-L.; Malliaras, G. G.; Anthony, J. E. *Chem. Commun.* **2011**, *47*, 7617–7619. (b) Tylleman, B.; Vande Velde, C. M. L.; Balandier, J.-Y.; Stas, S.; Sergeyev, S.; Geerts, Y. H. *Org. Lett.* **2011**, *13*, 5208–5211.

(6) For examples of the synthesis of isomerically pure naphthodithiophenes, see: (a) Shinamura, S.; Osaka, I.; Miyazaki, E.; Nakao, A.; Yamagishi, M.; Takeya, J.; Takimiya, K. *J. Am. Chem. Soc.* **2011**, *133*, 5024–5035. (b) Osaka, I.; Abe, T.; Shinamura, S.; Takimiya, K. *J. Am. Chem. Soc.* **2011**, *133*, 6852–6860. (c) Loser, S.; Bruns, C. J.; Miyauchi, H.; Ortiz, R. P.; Facchetti, A.; Stupp, S. I.; Marks, T. J. *J. Am. Chem. Soc.* **2011**, *133*, 8142–8145.

(7) While the stereochemistry about the olefins formed from the aldol condensation has not been assigned, NMR spectroscopic data suggest only one isomer.

(8) Quinone **11** has been previously synthesized as a mixture of *syn*- and *anti*-isomers using a significantly different approach; see: Reid, W.; Bender, H. *Chem. Ber.* **1956**, *89*, 1574–1577.

melting point (414 °C), which is followed immediately by decomposition. *i*-Bu_3Si- and *n*-Bu_3Si-substituted ABBTs **5b** and **5c** have progressively lower melting points, while their decomposition points are essentially identical. Finally, there is good agreement between the decomposition temperatures as measured by TGA and DSC analysis, indicating that thermal decomposition is accompanied by weight loss.

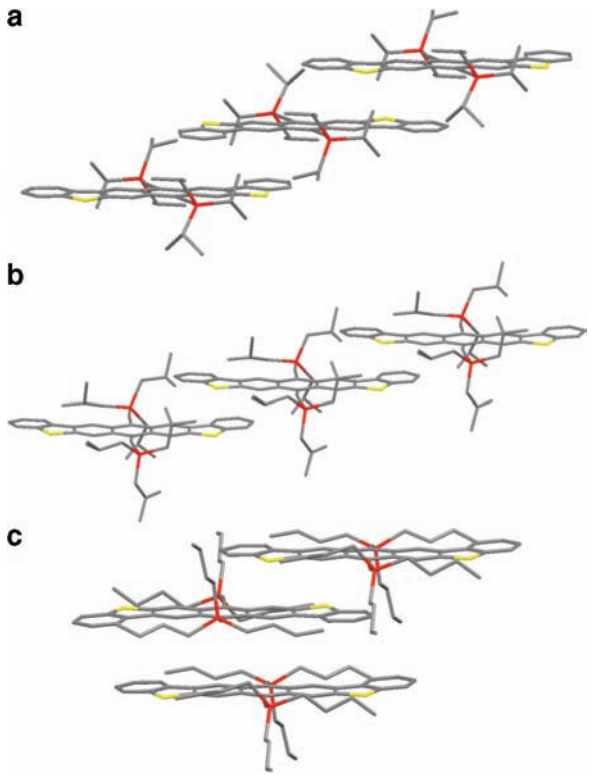

Figure 2. Solid-state packing of (a) **5a**, (b) **5b**, and (c) **5c**; carbon = gray, silicon = red, sulfur = yellow.

Not surprisingly, the shape and size of the pendent trialkylsilyl groups also impact the solid-state packing of ABBTs **5a**–**c** (Figure 2).[9] Single crystals for each compound have been obtained from CH_2Cl_2 solutions layered with acetone that were allowed to evaporate at 4 °C.[10] In the solid state, ABBTs **5a** and **5c** arrange as centrosymmetric dimeric pairs, with an interplanar spacing between adjacent molecules of the pair that is nearly identical for both structures (3.35–3.36 Å). The spacing that separates one dimeric pair from its neighbor is 3.40 Å for **5a** and 3.38 Å for **5c**. For both **5a** and **5c**, the dimeric pairs then form a 1-dimensional (1-D) slipped π-stacking arrangement. The π-stacked arrays of **5b**, on the other hand, afford 1-D channels with very limited acene overlap at an interplanar spacing of 3.44 Å. This is due to edge-to-face interactions by neighboring π-stacked channels, similar to the "sandwich herringbone" motif seen in pentacene semiconductors.

(9) Anthony, J. E.; Eaton, D. L.; Parkin, S. R. *Org. Lett.* **2002**, *4*, 15–18.

UV–vis absorption and emission spectra of **5a**–**c** were acquired in CH_2Cl_2 (Table 2), and maxima are identical within ±1 nm (representative spectra for **5c** are shown in Figure 3).[11] Briefly, ABBTs have a λ_{max} = 542 nm, which is blue-shifted by 13 nm compared to the analogous TIPS-ADT derivative, measured as a mixture of *syn*- and *anti*-isomers.[2c] Two weak mid-energy absorption bands are observed at λ = 442 and 417 nm, while in the UV region the most significant absorption band is found at λ = 350 nm. The emission spectra of **5a**–**c** show $\lambda_{max,em}$ at 548–549 nm. In each case, the Stokes shift is very small (6–7 nm, 202–235 cm^{-1}).

The λ_{max} values for **5a**–**c** taken from UV–vis spectra of thin films cast from CH_2Cl_2 all show a red shift versus the solution-state values. The bathochromic shift is largest for **5a** (36 nm), while smaller shifts of 15 nm and 6 nm are observed for **5c** and **5b**, respectively. The large red shift observed for **5a** is consistent with the solid-state packing from X-ray crystallographic analysis in which **5a** has improved π-stacking overlap compared to **5b** and **5c**.[11]

Cyclic voltammetry for **5a**–**c** establish the redox behavior and electrochemical gap, $E_g^{electro}$ (Table 2).[11] Within the electrochemical window scanned (1.0 to −1.8 V vs $Ag/AgNO_3$ electrode), only one oxidation (ca. 0.55 V vs Fc/Fc^+) and one reduction (ca. −1.68 V vs Fc/Fc^+) event are observed for each ABBT derivative, and all are reversible, except for the signals of **5a** which are quasi-reversible. The gap calculated from this data for **5a**–**c** (2.22–2.23 eV) is in good agreement with the optical HOMO–LUMO gaps of 2.21–2.22 eV estimated from solution-state UV–vis spectroscopy (Table 2).

Field effect transistors (FETs) based on thin films of **5b** and **5c** drop-cast from solution (1 wt % from toluene and chlorobenzene, respectively) provide for an evaluation of

(10) Crystallographic data for **5a** (CCDC 849435): $C_{48}H_{54}S_2Si_2$, M_r = 751.21; crystal dimensions (mm) 0.45 × 0.12 × 0.11; triclinic space group $P\bar{1}$ (No. 2); a = 11.317(2) Å, b = 12.747(3) Å, c = 15.369(3) Å; α = 75.186(3)°, β = 78.547(3)°, γ = 84.000(3)°; V = 2097.3(8) Å^3; Z = 2; ρ_{calcd} = 1.190 g cm^{-3}; μ = 0.216 mm^{-1}; λ = 0.71073 Å; T = −100 °C; $2\theta_{max}$ = 51.44°; total data collected = 15556; R_1 = 0.0540 [5019 observed reflections with $F_o^2 \geq 2\sigma(F_o^2)$]; w$R_2$ = 0.1530 for 469 variables, 7943 unique reflections, and five restraints; residual electron density = 0.415 and −0.362 e Å^{-3}. The C46A–C47A, C46A–C48A, C46B–C47B, and C46B–C48B distances within the disordered isopropyl group were constrained to be equal (within 0.03 Å) to a common refined value. The C47A···C48A and C47B···C48B distances were constrained to be equal (within 0.03 Å) during refinement. Crystallographic data for **5b** (CCDC 849436): $C_{54}H_{66}S_2Si_2$, M_r = 835.37; crystal dimensions (mm) 0.56 × 0.13 × 0.10; triclinic space group $P\bar{1}$ (No. 2); a = 11.1453(11) Å, b = 16.4944(16) Å, c = 26.181(3) Å; α = 88.4584(13)°, β = 85.4059(14)°, γ = 89.7663(13)°; V = 4795.7(8) Å^3; Z = 4; ρ_{calcd} = 1.157 g cm^{-3}; μ = 0.196 mm^{-1}; λ = 0.71073 Å; T = −100 °C; $2\theta_{max}$ = 51.80°; total data collected = 18532; R_1 = 0.0599 [12672 observed reflections with $F_o^2 \geq 2\sigma(F_o^2)$]; w$R_2$ = 0.1527 for 1295 variables, 18532 unique reflections, and 51 restraints; residual electron density = 0.598 and −0.602 e Å^{-3}. Distances involving the disordered triisobutylsilyl groups were restrained during refinement; see the Supporting Information. Crystallographic data for **5c** (CCDC 849437): $C_{54}H_{66}S_2Si_2$, M_r = 835.37; crystal dimensions (mm) 0.49 × 0.17 × 0.11; triclinic space group $P\bar{1}$ (No. 2); a = 8.9292(4) Å, b = 15.2194(6) Å, c = 18.4144(8) Å; α = 83.0261(5)°, β = 76.3552(5)°, γ = 88.7465(5)°; V = 2413.78(18) Å^3; Z = 2; ρ_{calcd} = 1.149 g cm^{-3}; μ = 0.194 mm^{-1}; λ = 0.71073 Å; T = −100 °C; $2\theta_{max}$ = 52.80°; total data collected = 19417; R_1 = 0.0451 [7756 observed reflections with $F_o^2 \geq 2\sigma(F_o^2)$]; w$R_2$ = 0.1395 for 560 variables and 9850 unique reflections; residual electron density = 0.619 and −0.376 e Å^{-3}.

(11) See the Supporting Information for details.

Table 2. Optoelectronic and Electrochemical Properties of ABBT **5a**–**c**

compd	λ_{max} (in CH_2Cl_2)/nm	λ_{max} (film)/nm[a]	λ_{onset} (film) /nm[a]	$\lambda_{max,em}$ (in CH_2Cl_2)/nm[b]	Stokes shift/nm	E_g^{opt} (in CH_2Cl_2)/eV[c]	$E_g^{electro}$ (in CH_2Cl_2)/eV[d]	E_{ox} (in CH_2Cl_2)/V[d]	E_{red} (in CH_2Cl_2)/V[d]
5a	542	578	613	548	6	2.22	2.23	0.55[e]	−1.68[e]
5b	542	548	624	549	7	2.21	2.23	0.54[f]	−1.69[f]
5c	542	557	613	548	6	2.22	2.22	0.55[f]	−1.67[f]

[a] Film from CH_2Cl_2. [b] Measured using λ_{exc} 504 nm. [c] The value used as the absorption edge corresponds to the lowest-energy absorption wavelength with a molar absorption coefficient $\varepsilon \geq 1000\ L \cdot mol^{-1} \cdot cm^{-1}$. [d] Cyclic voltammetry was performed in CH_2Cl_2 solutions containing 0.1 M n-Bu_4NPF_6 as supporting electrolyte. The potential values (E) were calculated using the following equation: $E = (E_{pc} + E_{pa})/2$, where E_{pc} and E_{pa} correspond to the cathodic and anodic peak potentials, respectively. Potentials are referenced to the ferrocene/ferrocenium (Fc/Fc^+) couple used as an internal standard. All potentials represent a one-electron reduction or oxidation event. [e] Measured at a scan rate of 200 $mV \cdot s^{-1}$. [f] Measured at a scan rate of 150 $mV \cdot s^{-1}$.

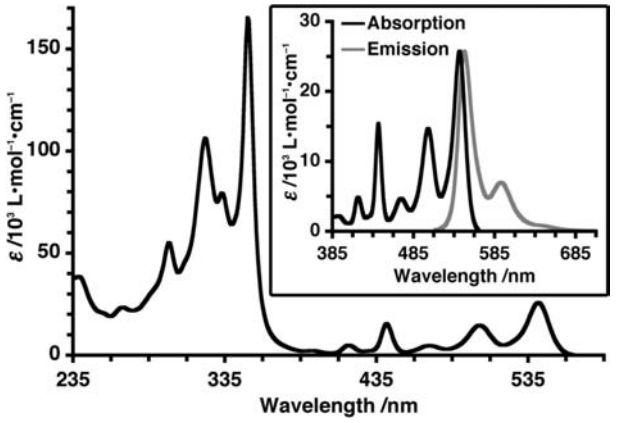

Figure 3. UV–vis spectrum of **5c** in CH_2Cl_2 (235–585 nm). Inset: expansion of low energy region of UV–vis absorption spectra (385–585 nm) and normalized emission spectra of **5c** in CH_2Cl_2 (510–710 nm) using $\lambda_{exc} = 504$ nm.

the charge transport properties. Because of low solubility and noncontinuous films, **5a** was not tested in FETs. For ABBTs **5b** and **5c**, both derivatives formed needle-like structures with poor coverage of the channel region of the device as expected from their 1-D π-stacked nature. ABBT **5c** exhibits reasonable hole transport considering the film morphology, with charge-carrier mobilities as high as $1.3 \times 10^{-2}\ cm^2/(V\ s)$. Hole mobilities for films of **5b** were lower, with a maximum of $2.2 \times 10^{-5}\ cm^2/(V\ s)$. The different behavior of **5b** and **5c** roughly correlates with the lesser degree of electronic interaction suggested by the solid-state UV-absorption spectrum (i.e., a smaller red shift vs solution-state data for **5b** relative to **5c**).[11]

In summary, a new class of heteroacene chromophores has been synthesized in isomerically pure form, namely the anthra[2,3-*b*:7,6-*b*']bis[1]benzothiophenes (*syn*-ABBTs. The choice of the ethynyl groups laterally appended to acene influences the thermal properties, as well as the solid-state packing. Finally, FETs fabricated from **5b** and **5c** afford moderate mobilities in the case of **5c**, consistent with better π-stacking suggested for this compound through the UV–vis analyses.

Acknowledgment. This work was supported by FAU Erlangen-Nürnberg and the Natural Sciences and Engineering Research Council of Canada (NSERC). D.L. thanks NSERC (PGS-D), the Alberta Ingenuity Fund, the University of Alberta, Alberta Heritage, and the Killam Trusts for scholarship support. J.E.A. and R.H. acknowledge the Office of Naval Research for support.

Supporting Information Available. Experimental procedures, spectroscopic data, ^1H and ^{13}C NMR spectra for all new compounds, and CIF files (**5a**–**c**). This material is available free of charge via the Internet at http://pubs.acs.org.